Part 1: Satellite Position Estimation Using Angle and Range Measurements

Let $\hat{m}$ and $\hat{s}$ be normalized units of position and time respectively, and let radians (rad) be the unit of angle. Let w and L be points representing the locations of a planet and a satellite orbiting said planet respectively, and let F_{A} be an inertial frame. Then, suppose that the planet doesn't move with respect to F_{A} and that the dynamics of the satellite are given by the Kepler problem equations, such that

$$\overset{\mathrm{A}\bullet\bullet}{\vec{r}}_{L/w}\Big|_{\mathrm{A}} = \frac{-\mu\ \vec{r}_{L/w}\big|_{\mathrm{A}}}{\left|\left|\vec{r}_{L/w}\big|_{\mathrm{A}}\right|\right|_2^3}, \tag{1}$$

where $\mu \in \mathbb{R}$ is given in $\hat{m}^3/\hat{s}^2$. Now, let

$$\vec{r}_{L/w}\big|_{\mathrm{A}} = \begin{bmatrix} X & Y & Z \end{bmatrix}^{\mathrm{T}}, \qquad \overset{\mathrm{A}\bullet}{\vec{r}}_{L/w}\Big|_{\mathrm{A}} = \begin{bmatrix} V_X & V_Y & V_Z \end{bmatrix}^{\mathrm{T}}, \tag{2}$$

where $X, Y, Z \in \mathbb{R}$ are given in $\hat{m}$ and $V_X, V_Y, V_Z \in \mathbb{R}$ are given in $\hat{m}/\hat{s}$, and define

$$\mathbb{X} \triangleq \begin{bmatrix} X & Y & Z & V_X & V_Y & V_Z \end{bmatrix}^{\mathrm{T}}. \tag{3}$$

Then, equation (1) can be rewritten as

$$\frac{d}{dt}\mathbb{X} = \begin{bmatrix} 0_{3\times3} & I_3 \\ \frac{-\mu}{\sqrt{X^2+Y^2+Z^2}^3} I_3 & 0_{3\times3} \end{bmatrix} \mathbb{X} = f(\mathbb{X}). \tag{4}$$

Next, let the equations resulting from linearizing and then discretizing equation (4) be given by

$$\mathbb{X}_{k+1} = e^{F(\mathbb{X}_k)T_{\mathrm{s}}}\mathbb{X}_k = A_k\mathbb{X}_k, \tag{5}$$

where $\mathbb{X}_k \in \mathbb{R}$ is the discretized version of $\mathbb{X}$ at step k, T_{s} is the sampling rate in $\hat{s}$, and $F\colon \mathbb{R}^3 \to \mathbb{R}^{6\times6}$ is the Jacobian of f, such that

$$F(\mathbb{X}_k) = \begin{bmatrix} 0_{3\times3} & I_3 \\ F_{X_k,Y_k,Z_k} & 0_{3\times3} \end{bmatrix}, \quad F_{X_k,Y_k,Z_k} = \begin{bmatrix} \frac{3\mu X_k^2}{r^5} - \frac{\mu}{r^3} & \frac{3\mu X_k Y_k}{r^5} & \frac{3\mu X_k Z_k}{r^5} \\ \frac{3\mu X_k Y_k}{r^5} & \frac{3\mu Y_k^2}{r^5} - \frac{\mu}{r^3} & \frac{3\mu Y_k Z_k}{r^5} \\ \frac{3\mu X_k Z_k}{r^5} & \frac{3\mu Y_k Z_k}{r^5} & \frac{3\mu Z_k^2}{r^5} - \frac{\mu}{r^3} \end{bmatrix}, \tag{6}$$

where $r = \sqrt{X_k^2 + Y_k^2 + Z_k^2}$. In order to account for acceleration uncertainties, a noise term is added to equation (5), such that

$$\mathbb{X}_{k+1} = A_k\mathbb{X}_k + \begin{bmatrix} 0_{3\times3} \\ 0.01\ I_3 \end{bmatrix} w_{1,k}, \tag{7}$$

where $w_{1,k} \sim \mathcal{N}(0_{3\times1}, I_3)$. Next, let the measurement model be given by

$$\mathbb{Y}_k = \begin{cases} g(\mathbb{X}_k) + 0.01\ I_3 w_{2,k}, & \mathrm{mod}(kT_{\mathrm{s}}, T_{\mathrm{meas}}) = 0, \\ 0_{3\times1}, & \text{otherwise}, \end{cases} \tag{8}$$

where $T_{\text{meas}} \in \mathbb{R}$ is the measurement rate given in $\hat{s}$, $w_{2,k} \sim \mathcal{N}(0_{3\times 1}, I_3)$, and

$$g(\mathbb{X}_k) = \begin{bmatrix} \rho_k \\ \text{az}_k \\ \text{el}_k \end{bmatrix} = \begin{bmatrix} g_1(\mathbb{X}_k) \\ g_2(\mathbb{X}_k) \\ g_3(\mathbb{X}_k) \end{bmatrix} = \begin{bmatrix} \sqrt{X_k^2 + Y_k^2 + Z_k^2} \\ -\arctan\frac{X_k}{Y_k} \\ \arctan\left(\frac{Z_k}{\sqrt{X_k^2+Y_k^2}}\right) \end{bmatrix}, \tag{9}$$

where ρ_k, az_k, and el_k are the range in $\hat{m}$, azimuth in rad, and elevation in rad of the satellite measured from w respectively.

Problem 1

a) Using equations (7) and (8), write the Kalman Filter (KF) equations to estimate $\mathbb{X}_k$.

b) Let $\hat{\mathbb{X}}_k$ be the estimate of $\mathbb{X}_k$ at time step k and suppose that $\mu = 0.4$, $\hat{\mathbb{X}}_0 = \begin{bmatrix} 2.5 & 0 & 1 & 0 & 0.5 & -0.1 \end{bmatrix}^{\text{T}}$, $P_{0|0} = I_6$, and that, for all $k > 0$, the range, azimuth, and elevation non-noisy measurements with sample time $0.01\hat{s}$ are given in the file AE584_Final_P1_meas_Ts_0_01.mat, such that $\rho_k = \text{Range}(k+1)$, $\text{az}_k = \text{Azimuth}(k+1)$, and $\text{el}_k = \text{Elevation}(k+1)$.

   For all $k \in \{0, 1, \ldots, 10000\}$, determine $\hat{\mathbb{X}}_k$ via an KF using the measurements in AE584_Final_P1_meas_Ts_0_01.mat for $T_{\text{s}} = 0.01\hat{s}$, and $T_{\text{meas}} \in \{1, 0.1\}\hat{s}$ (two sets of estimates). Justify your choices for Q_k and R_k (even if these are arbitrary). The file AE584_Final_P1_pos_Ts_0_01.mat contains the true trajectory of the satellite X_{ref}, Y_{ref}, and Z_{ref}. In one figure, use a 3D plot to plot the reference trajectory X_{ref}, Y_{ref}, and Z_{ref} and the estimated trajectories obtained for $T_{\text{meas}} = 1$ and $T_{\text{meas}} = 0.1\hat{s}$. In another figure, plot the 3 components of the reference trajectory and the estimated trajectories obtained for $T_{\text{meas}} = 1$ and $T_{\text{meas}} = 0.1\hat{s}$ versus normalized time in a 3-by-1 figure grid using the subplot function.

NOTE 1: The reference trajectory in file AE584_Final_P1_pos_Ts_0_01.mat was computed using $\mu = 0.5$, which is different form the one you are asked to use. This problem illustrates how the ˙ 'KF can handle inaccurate parameters used in the physical model.

NOTE 2: The azimuth angle in the AE584_Final_P1_meas_Ts_0_01.mat file has been unwrapped so that the values are continuous. This may cause issues when performing the corrector step in the KF since $g_2(\hat{\mathbb{X}}_{k+1|k})$ may yield wrapped azimuth angles. To address this, you can use the function AzUnwrap.m included in the project files on the output of $g_2(\hat{\mathbb{X}}_{k+1|k})$

and use $\mathbb{Y}_k - \begin{bmatrix} g_1(\hat{\mathbb{X}}_{k+1|k}) \\ \mathrm{AzUnwrap}(g_2(\hat{\mathbb{X}}_{k+1|k}), 0) \\ g_3(\hat{\mathbb{X}}_{k+1|k}) \end{bmatrix}$ instead of $\mathbb{Y}_k - \begin{bmatrix} g_1(\hat{\mathbb{X}}_{k+1|k}) \\ g_2(\hat{\mathbb{X}}_{k+1|k}) \\ g_3(\hat{\mathbb{X}}_{k+1|k}) \end{bmatrix}$ in the corrector step.

Otherwise, you could wrap the azimuth measurements and use the KF without the AzUnwrap function. This may cause sizeable oscillations when the azimuth measurements jump from π to $-\pi$ and viceversa, but as long as the estimates converge to the reference trajectory afterwards, this will be accepted.

NOTE 3: To calculate the arctangent in your code, use atan2, NOT atan.

Part 2: Planar Endoatmospheric Guidance

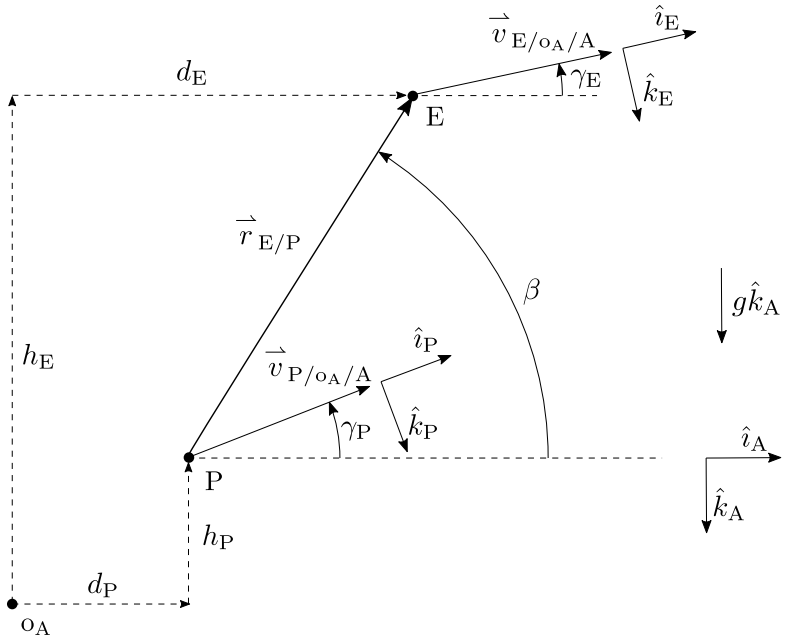

Figure 1: Planar interception geometry for the pursuer and evader. An inertial frame $\mathrm{F_A}$ is defined by the unit vectors $\hat{\imath}_{\mathrm{A}}, \hat{k}_{\mathrm{A}}$. The pursuer P and evader E, are at altitudes h_{P} and h_{E}, respectively, relative to $\mathrm{o_A}$, which is a fixed point at sea level. P and E are distances d_{P} and d_{E} downrange, respectively. The line-of-sight vector $\vec{r}_{\mathrm{E/P}}$ makes the line-of-sight angle β relative to $\hat{\imath}_{\mathrm{A}}$. The unit vectors $\hat{\imath}_{\mathrm{P}}$ and $\hat{\imath}_{\mathrm{E}}$ are aligned with $\vec{v}_{\mathrm{P/o_A/A}}$ and $\vec{v}_{\mathrm{E/o_A/A}}$, respectively. The gravity vector $g\hat{k}_{\mathrm{A}}$ affects all dynamic motion.

Consider a pursuer P and evader E, with position vectors $\vec{r}_{\mathrm{P/o_A}}$ and $\vec{r}_{\mathrm{E/o_A}}$, respectively, where $\mathrm{o_A}$ is a reference point with zero inertial acceleration. Let the pursuer and evader speeds V_{P} and V_{E}, respectively, be given by

$$V_{\mathrm{P}} \triangleq |\vec{v}_{\mathrm{P/o_A/A}}|, \quad V_{\mathrm{E}} \triangleq |\vec{v}_{\mathrm{E/o_A/A}}|. \tag{10}$$

Let $\mathrm{F_P}$ and $\mathrm{F_E}$ be frames whose x-axes are aligned with the velocity vectors of the pursuer and evader, respectively, and thus

$$\vec{v}_{\mathrm{P/o_A/A}} = V_{\mathrm{P}}\hat{\imath}_{\mathrm{P}}, \quad \vec{v}_{\mathrm{E/o_A/A}} = V_{\mathrm{E}}\hat{\imath}_{\mathrm{E}}, \tag{11}$$

and

$$\mathrm{F_A} \xrightarrow[2]{\gamma_{\mathrm{P}}} \mathrm{F_P}, \quad \mathrm{F_A} \xrightarrow[2]{\gamma_{\mathrm{E}}} \mathrm{F_E}, \tag{12}$$

where γ_{P} and γ_{E} are the pursuer and evader flight-path angles, respectively, and

$$\vec{\omega}_{\mathrm{P/A}} = \dot{\gamma}_{\mathrm{P}}\hat{\jmath}_{\mathrm{P}}, \quad \vec{\omega}_{\mathrm{E/A}} = \dot{\gamma}_{\mathrm{E}}\hat{\jmath}_{\mathrm{E}}. \tag{13}$$

Taking the time derivative of (11) with respect to the $\mathrm{F_A}$ frame yields

$$\vec{a}_{\mathrm{P/o_A/A}} = \dot{V}_{\mathrm{P}}\hat{\imath}_{\mathrm{P}} + V_{\mathrm{P}}\overset{\mathrm{A}\bullet}{\hat{\imath}}_{\mathrm{P}}, \quad \vec{a}_{\mathrm{E/o_A/A}} = \dot{V}_{\mathrm{E}}\hat{\imath}_{\mathrm{E}} + V_{\mathrm{E}}\overset{\mathrm{A}\bullet}{\hat{\imath}}_{\mathrm{E}}, \tag{14}$$

$$\vec{a}_{\mathrm{P/o_A/A}} = \dot{V}_{\mathrm{P}}\hat{\imath}_{\mathrm{P}} + V_{\mathrm{P}}(\vec{\omega}_{\mathrm{P/A}} \times \hat{\imath}_{\mathrm{P}}), \quad \vec{a}_{\mathrm{E/o_A/A}} = \dot{V}_{\mathrm{E}}\hat{\imath}_{\mathrm{E}} + V_{\mathrm{E}}(\vec{\omega}_{\mathrm{E/A}} \times \hat{\imath}_{\mathrm{E}}), \tag{15}$$

$$\vec{a}_{\mathrm{P/o_A/A}} = \dot{V}_{\mathrm{P}}\hat{\imath}_{\mathrm{P}} + V_{\mathrm{P}}(\dot{\gamma}_{\mathrm{P}}\hat{\jmath}_{\mathrm{P}} \times \hat{\imath}_{\mathrm{P}}), \quad \vec{a}_{\mathrm{E/o_A/A}} = \dot{V}_{\mathrm{E}}\hat{\imath}_{\mathrm{E}} + V_{\mathrm{E}}(\dot{\gamma}_{\mathrm{E}}\hat{\jmath}_{\mathrm{E}} \times \hat{\imath}_{\mathrm{E}}), \tag{16}$$

$$\vec{a}_{\mathrm{P/o_A/A}} = \dot{V}_{\mathrm{P}}\hat{\imath}_{\mathrm{P}} - V_{\mathrm{P}}\dot{\gamma}_{\mathrm{P}}\hat{k}_{\mathrm{P}}, \quad \vec{a}_{\mathrm{E/o_A/A}} = \dot{V}_{\mathrm{E}}\hat{\imath}_{\mathrm{E}} - V_{\mathrm{E}}\dot{\gamma}_{\mathrm{E}}\hat{k}_{\mathrm{E}}. \tag{17}$$

Kinematic Engagement

Let $\dot{V}_{\mathrm{E}} = \dot{V}_{\mathrm{P}} = 0$, $g = 0$, and assume that

$$\vec{a}_{\mathrm{P/o_A/A}} = n_{z,\mathrm{P}}\hat{k}_{\mathrm{P}}, \quad \vec{a}_{\mathrm{E/o_A/A}} = n_{z,\mathrm{E}}\hat{k}_{\mathrm{E}}. \tag{18}$$

Then the kinematic differential equations for the engagement are

$$\dot{h}_{\mathrm{P}} = V_{\mathrm{P}} \sin\gamma_{\mathrm{P}}, \tag{19}$$

$$\dot{d}_{\mathrm{P}} = V_{\mathrm{P}} \cos\gamma_{\mathrm{P}}, \tag{20}$$

$$\dot{\gamma}_{\mathrm{P}} = -\frac{1}{V_{\mathrm{P}}} n_{z,\mathrm{P}}, \tag{21}$$

$$\dot{h}_{\mathrm{E}} = V_{\mathrm{E}} \sin\gamma_{\mathrm{E}}, \tag{22}$$

$$\dot{d}_{\mathrm{E}} = V_{\mathrm{E}} \cos\gamma_{\mathrm{E}}, \tag{23}$$

$$\dot{\gamma}_{\mathrm{E}} = -\frac{1}{V_{\mathrm{E}}} n_{z,\mathrm{E}}, \tag{24}$$

$$\dot{R} = V_{\mathrm{E}} \cos(\beta - \gamma_{\mathrm{E}}) - V_{\mathrm{P}} \cos(\beta - \gamma_{\mathrm{P}}), \tag{25}$$

$$\dot{\beta} = \frac{V_{\mathrm{P}} \sin(\beta - \gamma_{\mathrm{P}}) - V_{\mathrm{E}} \sin(\beta - \gamma_{\mathrm{E}})}{R}, \tag{26}$$

where $h_{\mathrm{P}}, d_{\mathrm{P}}$, and $h_{\mathrm{E}}, d_{\mathrm{E}}$, are the altitude and downrange distance of the pursuer and evader, respectively, R is the range, and β is the line-of-sight angle.

Dynamic Engagement

Let the acceleration of the pursuer and evader be given by

$$\vec{a}_{\mathrm{P/o_A/A}} = (\tfrac{T_{\mathrm{P}} - D_{\mathrm{P}}}{m_{\mathrm{P}}} - g\sin\gamma_{\mathrm{P}})\hat{\imath}_{\mathrm{P}} + (n_{z,\mathrm{P}} + g\cos\gamma_{\mathrm{P}})\hat{k}_{\mathrm{P}}, \tag{27}$$

$$\vec{a}_{\mathrm{E/o_A/A}} = (\tfrac{T_{\mathrm{E}} - D_{\mathrm{E}}}{m_{\mathrm{E}}} - g\sin\gamma_{\mathrm{E}})\hat{\imath}_{\mathrm{E}} + (n_{z,\mathrm{E}} + g\cos\gamma_{\mathrm{E}})\hat{k}_{\mathrm{E}}, \tag{28}$$

respectively, where $T_{\mathrm{P}}, D_{\mathrm{P}}, m_{\mathrm{P}}, n_{z,\mathrm{P}}$ and $T_{\mathrm{E}}, D_{\mathrm{E}}, m_{\mathrm{E}}, n_{z,\mathrm{E}}$ are the thrust force, drag force, mass, and normal acceleration of the pursuer and evader, respectively. Note that the inclusion of mass, thrust force, drag force, and acceleration due to gravity implies that we are describing the dynamics (and not just the kinematics) of the engagement.

It follows from (17), (27), and (28) that

$$\dot{V}_{\mathrm{P}} = \tfrac{T_{\mathrm{P}} - D_{\mathrm{P}}}{m_{\mathrm{P}}} - g \sin \gamma_{\mathrm{P}}, \tag{29}$$

$$\dot{V}_{\mathrm{E}} = \tfrac{T_{\mathrm{E}} - D_{\mathrm{E}}}{m_{\mathrm{E}}} - g \sin \gamma_{\mathrm{E}}, \tag{30}$$

$$\dot{\gamma}_{\mathrm{P}} = -\tfrac{1}{V_{\mathrm{P}}}(n_{z,\mathrm{P}} + g \cos \gamma_{\mathrm{P}}), \tag{31}$$

$$\dot{\gamma}_{\mathrm{E}} = -\tfrac{1}{V_{\mathrm{E}}}(n_{z,\mathrm{E}} + g \cos \gamma_{\mathrm{E}}). \tag{32}$$

Assuming that the angle of attack is zero, the drag force on the pursuer and evader are given by

$$D_{\mathrm{P}} = \tfrac{1}{2}\rho(h_{\mathrm{P}}) V_{\mathrm{P}}^2 S_{\mathrm{P}} C_{\mathrm{d,P}}(\mathrm{M}_{\mathrm{P}}), \tag{33}$$

$$D_{\mathrm{E}} = \tfrac{1}{2}\rho(h_{\mathrm{E}}) V_{\mathrm{E}}^2 S_{\mathrm{E}} C_{\mathrm{d,E}}(\mathrm{M}_{\mathrm{E}}), \tag{34}$$

respectively, where M_{P} and M_{E} are the Mach numbers at altitudes h_{P} and h_{E}, respectively, as given by the international standard atmosphere (ISA). Note that the Mach number M at the altitude h is given by $\mathrm{M}(h) = \frac{V}{a(h)}$, where V is the speed and $a(h)$ is the speed of sound at the altitude h.

Sensor Outputs

The seeker provides measurements R of the magnitude of the line-of-sight vector $\vec{r}_{\mathrm{E/P}}$

$$R \triangleq |\vec{r}_{\mathrm{E/P}}| = \sqrt{(h_{\mathrm{E}} - h_{\mathrm{P}})^2 + (d_{\mathrm{E}} - d_{\mathrm{P}})^2}. \tag{35}$$

Additionally, the seeker provides measurements of

$$\dot{R} = \frac{(h_{\mathrm{E}} - h_{\mathrm{P}})(\dot{h}_{\mathrm{E}} - \dot{h}_{\mathrm{P}}) + (d_{\mathrm{E}} - d_{\mathrm{P}})(\dot{d}_{\mathrm{E}} - \dot{d}_{\mathrm{P}})}{\sqrt{(h_{\mathrm{E}} - h_{\mathrm{P}})^2 + (d_{\mathrm{E}} - d_{\mathrm{P}})^2}}, \tag{36}$$

$$= \frac{(h_{\mathrm{E}} - h_{\mathrm{P}})(V_{\mathrm{E}} \sin \gamma_{\mathrm{E}} - V_{\mathrm{P}} \sin \gamma_{\mathrm{P}}) + (d_{\mathrm{E}} - d_{\mathrm{P}})(V_{\mathrm{E}} \cos \gamma_{\mathrm{E}} - V_{\mathrm{P}} \cos \gamma_{\mathrm{P}})}{\sqrt{(h_{\mathrm{E}} - h_{\mathrm{P}})^2 + (d_{\mathrm{E}} - d_{\mathrm{P}})^2}}. \tag{37}$$

The line-of-sight angle is defined to be

$$\beta \triangleq \theta_{\vec{r}_{\mathrm{E/P}}/\hat{\imath}_{\mathrm{A}}/\hat{\jmath}_{\mathrm{A}}} \tag{38}$$

$$= \mathrm{atan2}(h_{\mathrm{E}} - h_{\mathrm{P}}, d_{\mathrm{E}} - d_{\mathrm{P}}). \tag{39}$$

The seeker also provides measurements of the line-of-sight-angle rate

$$\dot{\beta} = \frac{1}{1 + (\frac{h_{\mathrm{E}} - h_{\mathrm{P}}}{d_{\mathrm{E}} - d_{\mathrm{P}}})^2} \frac{(d_{\mathrm{E}} - d_{\mathrm{P}})(\dot{h}_{\mathrm{E}} - \dot{h}_{\mathrm{P}}) - (h_{\mathrm{E}} - h_{\mathrm{P}})(\dot{d}_{\mathrm{E}} - \dot{d}_{\mathrm{P}})}{(d_{\mathrm{E}} - d_{\mathrm{P}})^2} \tag{40}$$

$$= \frac{(d_{\mathrm{E}} - d_{\mathrm{P}})^2}{(d_{\mathrm{E}} - d_{\mathrm{P}})^2 + (h_{\mathrm{E}} - h_{\mathrm{P}})^2} \frac{(d_{\mathrm{E}} - d_{\mathrm{P}})(\dot{h}_{\mathrm{E}} - \dot{h}_{\mathrm{P}}) - (h_{\mathrm{E}} - h_{\mathrm{P}})(\dot{d}_{\mathrm{E}} - \dot{d}_{\mathrm{P}})}{(d_{\mathrm{E}} - d_{\mathrm{P}})^2} \tag{41}$$

$$= \frac{(d_{\mathrm{E}} - d_{\mathrm{P}})(V_{\mathrm{E}} \sin \gamma_{\mathrm{E}} - V_{\mathrm{P}} \sin \gamma_{\mathrm{P}}) - (h_{\mathrm{E}} - h_{\mathrm{P}})(V_{\mathrm{E}} \cos \gamma_{\mathrm{E}} - V_{\mathrm{P}} \cos \gamma_{\mathrm{P}})}{(d_{\mathrm{E}} - d_{\mathrm{P}})^2 + (h_{\mathrm{E}} - h_{\mathrm{P}})^2}. \tag{42}$$

Equations of Motion

The dynamic differential equations for the engagement are

$$\dot{x} = f(x, u, w), \tag{43}$$

$$y = h(x), \tag{44}$$

where

$$x \triangleq \begin{bmatrix} V_{\mathrm{P}} \\ \gamma_{\mathrm{P}} \\ h_{\mathrm{P}} \\ d_{\mathrm{P}} \\ V_{\mathrm{E}} \\ \gamma_{\mathrm{E}} \\ h_{\mathrm{E}} \\ d_{\mathrm{E}} \end{bmatrix}, \quad w \triangleq \begin{bmatrix} T_{\mathrm{P}} \\ n_{z,\mathrm{E}} \end{bmatrix}, \quad u \triangleq n_{z,\mathrm{P}}, \quad f(x,u,w) \triangleq \begin{bmatrix} \frac{T_{\mathrm{P}} - \frac{1}{2}\rho(h_{\mathrm{P}})V_{\mathrm{P}}^2 S_{\mathrm{P}} C_{\mathrm{d,P}}(\mathrm{M_P})}{m_{\mathrm{P}}} - g\sin\gamma_{\mathrm{P}} \\ -\frac{1}{V_{\mathrm{P}}}(n_{z,\mathrm{P}} + g\cos\gamma_{\mathrm{P}}) \\ V_{\mathrm{P}}\sin\gamma_{\mathrm{P}} \\ V_{\mathrm{P}}\cos\gamma_{\mathrm{P}} \\ \frac{T_{\mathrm{E}} - \frac{1}{2}\rho(h_{\mathrm{E}})V_{\mathrm{E}}^2 S_{\mathrm{E}} C_{\mathrm{d,E}}(\mathrm{M_E})}{m_{\mathrm{E}}} - g\sin\gamma_{\mathrm{E}} \\ -\frac{1}{V_{\mathrm{E}}}(n_{z,\mathrm{E}} + g\cos\gamma_{\mathrm{E}}) \\ V_{\mathrm{E}}\sin\gamma_{\mathrm{E}} \\ V_{\mathrm{E}}\cos\gamma_{\mathrm{E}} \end{bmatrix}, \tag{45}$$

$$y \triangleq \begin{bmatrix} R \\ \dot{R} \\ \dot{\beta} \end{bmatrix}, \quad h(x) \triangleq \begin{bmatrix} \sqrt{(h_{\mathrm{E}} - h_{\mathrm{P}})^2 + (d_{\mathrm{E}} - d_{\mathrm{P}})^2} \\ \frac{(h_{\mathrm{E}} - h_{\mathrm{P}})(V_{\mathrm{E}}\sin\gamma_{\mathrm{E}} - V_{\mathrm{P}}\sin\gamma_{\mathrm{P}}) + (d_{\mathrm{E}} - d_{\mathrm{P}})(V_{\mathrm{E}}\cos\gamma_{\mathrm{E}} - V_{\mathrm{P}}\cos\gamma_{\mathrm{P}})}{\sqrt{(h_{\mathrm{E}} - h_{\mathrm{P}})^2 + (d_{\mathrm{E}} - d_{\mathrm{P}})^2}} \\ \frac{(d_{\mathrm{E}} - d_{\mathrm{P}})(V_{\mathrm{E}}\sin\gamma_{\mathrm{E}} - V_{\mathrm{P}}\sin\gamma_{\mathrm{P}}) - (h_{\mathrm{E}} - h_{\mathrm{P}})(V_{\mathrm{E}}\cos\gamma_{\mathrm{E}} - V_{\mathrm{P}}\cos\gamma_{\mathrm{P}})}{(d_{\mathrm{E}} - d_{\mathrm{P}})^2 + (h_{\mathrm{E}} - h_{\mathrm{P}})^2} \end{bmatrix}. \tag{46}$$

For realism we assume that $|n_{z,\mathrm{E}}| < 8\,\mathrm{g}$ and $|n_{z,\mathrm{P}}| < 40\,\mathrm{g}$, where g is the acceleration due to gravity in $\mathrm{m/s^2}$. T_{P} is is given as an explicit function of time since it represents the thrust profile of a solid rocket motor. We assume that T_{P} is independent of altitude h_{P}. We do not consider air-breathing propulsion systems, including air-augmented rockets. T_{E} and $n_{z,\mathrm{E}}$ are given as explicit functions of time since they are unknown to the pursuer. $\rho(h)$ is the density of air at altitude h given by ISA. The drag coefficients $C_{\mathrm{d,P}}(\mathrm{M_P})$ and $C_{\mathrm{d,E}}(\mathrm{M_E})$ are functions of Mach number which is computed using the vehicle speed and the local speed of sound at an altitude given by ISA.

Pursuer and Evader Models

Pursuer Model

Let the pursuer be an AIM120C5 beyond-visual-range (BVR) air-to-air missile, also known as the advanced medium-range air-to-air missile (AMRAAM). For simplicity we assume that AMRAAM has a constant mass $m_{\mathrm{P}} = 130$ kg, which corresponds to its mass with half of its rocket fuel. We assume that AMRAAM is equipped with a boost-sustain rocket motor whose

thrust is given by

$$T_{\mathrm{P}}(t) = \begin{cases} 11,000 \text{ N}, & 0 \text{ s} \leq t < 10 \text{ s}, \\ 1,800 \text{ N}, & 10 \text{ s} \leq t < 30 \text{ s}, \\ 0 \text{ N}, & t > 30 \text{ s}. \end{cases} \tag{47}$$

The drag coefficient of the pursuer $C_{\mathrm{d,P}}(\mathrm{M_P})$ is given by

$$C_{\mathrm{d,P}}(\mathrm{M_P}) = \mathrm{pchip}(\mathrm{M_{P,i}}, C_{\mathrm{d,P,i}}, \mathrm{M_P}), \tag{48}$$

where pchip is the MATLAB function that implements a piecewise cubic Hermite interpolating polynomial fit to the data $M_{\mathrm{P,i}}, C_{\mathrm{d,P,i}}$, and

$$\mathrm{M_{P,i}} = \begin{bmatrix} 0 & 0.6 & 0.8 & 1 & 1.2 & 2 & 3 & 4 & 5 \end{bmatrix}, \tag{49}$$

$$C_{\mathrm{d,P,i}} = \begin{bmatrix} 0.016 & 0.016 & 0.0195 & 0.045 & 0.039 & 0.0285 & 0.024 & 0.0215 & 0.020 \end{bmatrix}. \tag{50}$$

Figure 2 shows $C_{\mathrm{d,P}}(\mathrm{M_P})$ versus $\mathrm{M_P}$. The values of $C_{\mathrm{d,P}}(\mathrm{M_P})$ are given with respect to $S_{\mathrm{P}} = 2.3 \text{ m}^2$.

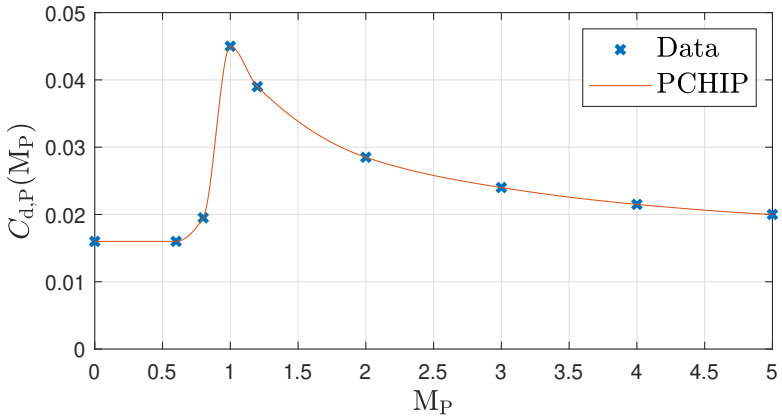

Figure 2: $C_{\mathrm{d,P}}(\mathrm{M_P})$ versus $\mathrm{M_P}$.

Evader Model

Let the evader be an F-16 fighter jet. For simplicity we assume that the F-16 has a constant mass $m_{\mathrm{E}} = 10000$ kg. Let the thrust for the F-16 be given by

$$T_{\mathrm{E}}(h_{\mathrm{E}}) = \frac{\rho(h_{\mathrm{E}})}{\rho(0)} 76310 \text{ N}, \tag{51}$$

which is an approximation of the maximum dry thrust at the altitude h_{E}. The drag coefficient of the evader $C_{\mathrm{d,E}}(\mathrm{M_E})$ is given by

$$C_{\mathrm{d,E}}(\mathrm{M_E}) = \mathrm{pchip}(\mathrm{M_{E,i}}, C_{\mathrm{d,E,i}}, \mathrm{M_E}), \tag{52}$$

where

$$\mathrm{M_{E,i}} = \begin{bmatrix} 0 & 0.9 & 1 & 1.2 & 1.6 & 2 \end{bmatrix}, \tag{53}$$

$$C_{\mathrm{d,E,i}} = \begin{bmatrix} 0.0175 & 0.019 & 0.05 & 0.045 & 0.043 & 0.038 \end{bmatrix}. \tag{54}$$

The values of $C_{\mathrm{d,E}}(\mathrm{M_E})$ are given with respect to $S_{\mathrm{E}} = 28\ \mathrm{m}^2$. Figure 3 shows $C_{\mathrm{d,E}}(\mathrm{M_E})$ versus $\mathrm{M_E}$.

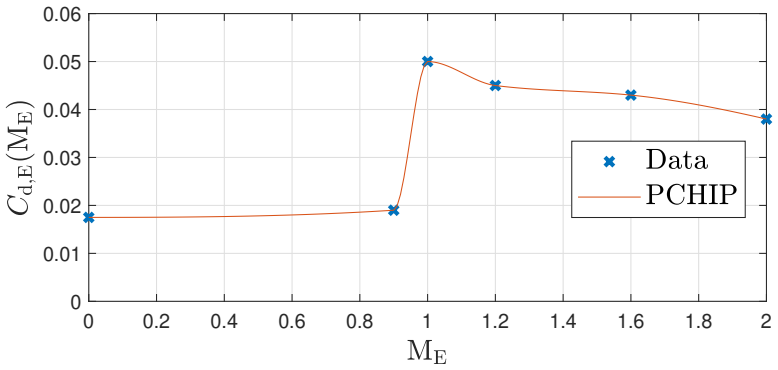

Figure 3: $C_{\mathrm{d,E}}(\mathrm{M_E})$ versus $\mathrm{M_E}$.

Optimal Guidance

At time t, let the discretization of (43) be given by

$$x_{k+1} = x_k + T_{\mathrm{s}} \cdot f(x_k, u_k, w_k), \tag{55}$$

where all signals are discretized as $x_k \triangleq x(t + kT_{\mathrm{s}})$, and thus x_0 represents the sampled value of $x(t)$, as opposed to the sampled value of $x(0)$. Note that the time t represents the current time as opposed to the launch time. The goal of the optimal guidance law is to achieve the minimum miss distance in the least amount of time.

The minimum miss distance and intercept-time optimization can be expressed as

$$\min_{U_N \in \mathbb{R}^{N+1}} R(t + NT_{\mathrm{s}})^2 + T_{\mathrm{s}}^2, \tag{56}$$

subject to

$$T_{\mathrm{s}} > 0, \tag{57}$$

$$x_{k+1} - x_k - T_{\mathrm{s}} \cdot f(x_k, u_k, w_k) = 0, \tag{58}$$

$$|u_k| < 40\,\mathrm{g}, \tag{59}$$

for $k = 0, \ldots, N-1$, where

$$U_N \triangleq \begin{bmatrix} n_{z,\mathrm{P}}(t+T_\mathrm{s}) \\ \vdots \\ n_{z,\mathrm{P}}(t+NT_\mathrm{s}) \\ T_\mathrm{s} \end{bmatrix} \in \mathbb{R}^{N+1}, \tag{60}$$

Note that the time-to-go $t_{\mathrm{go}} \triangleq NT_\mathrm{s}$ is a function of N and T_s. Since N is fixed, a smaller value of T_s corresponds to a smaller time-to-go. Furthermore, $R(t+NT_\mathrm{s})$ is the miss distance at $t+t_{\mathrm{go}}$. The optimization (56) is performed at each update of the guidance law and the first element $n_{z,\mathrm{P}}(t+T_\mathrm{s})$ of U_N is applied at the next step.

Simulation of Optimal Guidance

Let $\gamma_\mathrm{E}(0) = 0$ rad, $d_\mathrm{E}(0) = 5500$ m, and $n_{z,\mathrm{E}} = -\mathrm{g}$. The engagement is simulated for $0 \text{ s} \leq t \leq 50$ s by using the dynamic differential equations (45) and (46) with the gravity-corrected proportional guidance law and the optimal guidance law with $N = 4$. It is assumed that at each time t, the entire state $x(t+0\cdot T_\mathrm{s}) = x_0$ and the evader normal acceleration $n_{z,\mathrm{E}}$ are known. The gravity-corrected proportional guidance law failed to intercept the evader and

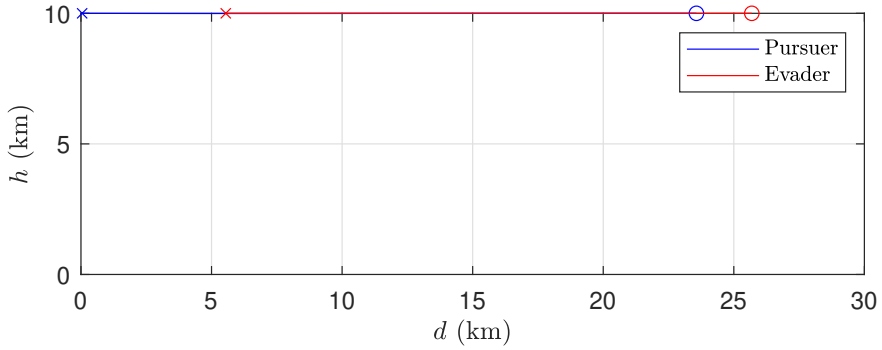

Figure 4: Pursuer and evader trajectories for gravity-corrected proportional guidance law.

the interception time for the optimal guidance law is 25.6 s.

The pursuer with the optimal guidance law climbs to altitude and utilizes the pursuer's boost thrust to gain gravitational potential energy. Furthermore, at higher altitude, the rarer atmosphere allows the pursuer to gain more speed for the same thrust profile. Towards the end of the intercept the pursuer dives down towards the target, converting the potential energy to speed. This maneuver is called *lofting*. This speed advantage is demonstrated by Figure 7.

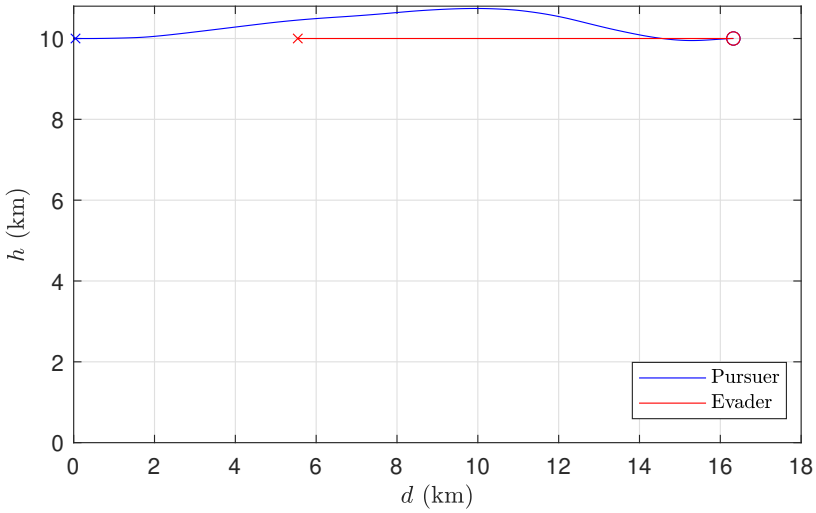

Figure 5: Pursuer and evader trajectories for optimal guidance law.

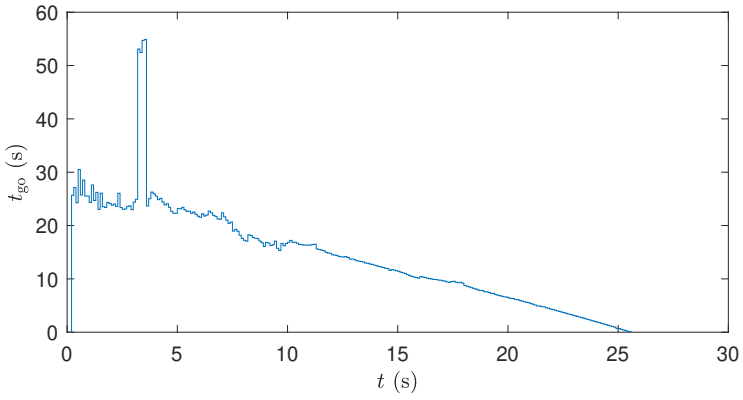

Figure 6: t_{go} versus t for the optimal guidance law.

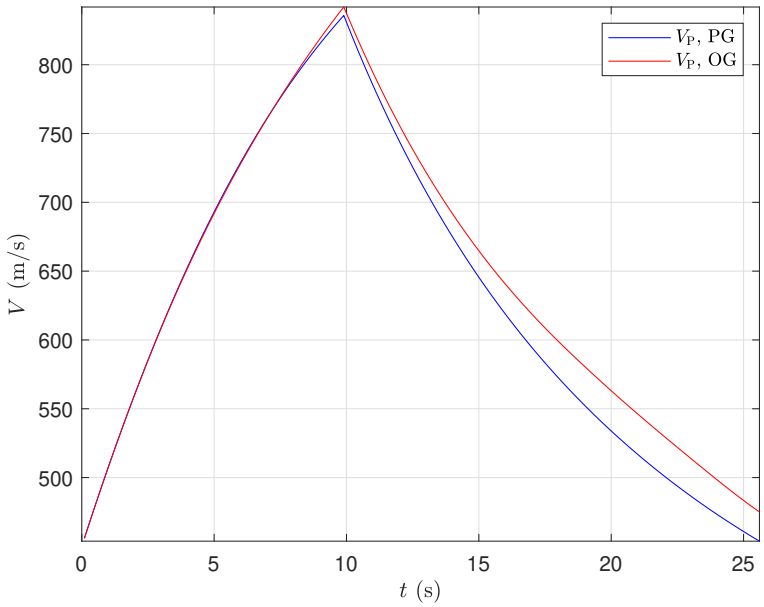

Figure 7: Pursuer speeds for proportional and optimal guidance laws.

Problems

NOTE: You should not present pdf files with your code for these problems. Just upload your code in the zip file.

Unless stated otherwise, for all problems let $V_{\mathrm{P}}(0) = 450\ \mathrm{m/s}$, $\gamma_{\mathrm{P}}(0) = 0\ \mathrm{rad}$, $h_{\mathrm{P}}(0) = 10000\ \mathrm{m}$, $d_{\mathrm{P}}(0) = 0\ \mathrm{m}$, $V_{\mathrm{E}}(0) = 450\ \mathrm{m/s}$, $\gamma_{\mathrm{E}}(0) = \pi\ \mathrm{rad}$, $h_{\mathrm{E}}(0) = 10000\ \mathrm{m}$, and $d_{\mathrm{E}}(0) = 30000\ \mathrm{m}$. This initial condition for (45) represents a typical high-altitude BVR engagement scenario. Terminate the engagement simulation if at least one of the following fuzing conditions is satisfied:

$i)$ $t > 500$ s,
$ii)$ $R(t) < 10$ m and either $R(t)$ crosses 0 or $\dot{R}(t) > 0$,
$iii)$ $h_{\mathrm{P}}(t) < 0$,
$iv)$ $h_{\mathrm{E}}(t) < 0$,
$v)$ $V_{\mathrm{P}}(t) < 0$,
$vi)$ $V_{\mathrm{E}}(t) < 0$.

The miss distance is defined to be the value of R at the end of the simulation. Use ode45 to simulate engagements and ensure that measurements are available every $T_{\mathrm{s}} = 0.1$ s. Furthermore, select $T_{\mathrm{s}} = 0.1$ s for the optimal guidance law update.
Note: Skeleton code is provided for problems 2–4.

Problem 2.

$i)$ Simulate the engagement by using the kinematic differential equations (19)–(26) with the constant speeds $V_{\mathrm{P}}(t) = 900\ \mathrm{m/s}$, $V_{\mathrm{E}}(t) = 450\ \mathrm{m/s}$, and

$$n_{z,\mathrm{E}}(t) = \begin{cases} -8\,\mathrm{g}, & 0\ \mathrm{s} \le t < 9\ \mathrm{s}, \\ 0\,\mathrm{g}, & 9\ \mathrm{s} \le t < 10\ \mathrm{s}, \\ -6\,\mathrm{g}, & 10\ \mathrm{s} \le t < 22\ \mathrm{s}, \\ 0\,\mathrm{g}, & t \ge 22\ \mathrm{s}. \end{cases} \tag{61}$$

Use the proportional guidance law

$$n_{z,\mathrm{P}} = -3|\dot{R}|\dot{\beta}, \tag{62}$$

subject to

$$|n_{z,\mathrm{P}}| < 40\,\mathrm{g}. \tag{63}$$

On the same axes plot the trajectories of the pursuer and evader in blue and red, respectively. What is the miss distance?

ii) Simulate the engagement by using the dynamic differential equations (43)–(46) with

$$n_{z,\mathrm{E}}(t) = \begin{cases} -6\,\mathrm{g}, & 0\ \mathrm{s} \leq t < 26\ \mathrm{s}, \\ -\mathrm{g}, & t \geq 26\ \mathrm{s}. \end{cases} \tag{64}$$

Use the gravity-corrected proportional guidance law

$$n_{z,\mathrm{P}} = -3|\dot{R}|\dot{\beta} - g\cos\gamma_{\mathrm{P}}, \tag{65}$$

subject to

$$|n_{z,\mathrm{P}}| < 40\,\mathrm{g}. \tag{66}$$

On the same axes plot the trajectories of the pursuer and evader in blue and red, respectively. On the same axes plot the pursuer and evader speeds in blue and red, respectively. What is the miss distance?

iii) Explain the differences in the miss distances obtained using the kinematics and dynamics engagement simulations.

Problem 3. Simulate the engagement by using the dynamic differential equations (43)–(46) with the gravity-corrected proportional guidance law

$$n_{z,\mathrm{P}} = -3|\dot{R}|\dot{\beta} - g\cos\gamma_{\mathrm{P}}, \tag{67}$$

subject to

$$|n_{z,\mathrm{P}}| < 40\,\mathrm{g}, \tag{68}$$

where the evader maneuvers as

$i)$

$$n_{z,\mathrm{E}}(t) = \begin{cases} 4\,\mathrm{g}, & 0\ \mathrm{s} \le t < 10\ \mathrm{s}, \\ -3\,\mathrm{g}, & 10\ \mathrm{s} \le t < 29\ \mathrm{s}, \\ 3\,\mathrm{g}, & 29\ \mathrm{s} \le t < 70\ \mathrm{s}, \\ -0.5\,\mathrm{g}, & 70\ \mathrm{s} \le t < 89\ \mathrm{s}, \\ \mathrm{g}, & t \ge 89\ \mathrm{s}. \end{cases} \tag{69}$$

$ii)$

$$n_{z,\mathrm{E}}(t) = \begin{cases} 5\,\mathrm{g}, & 0\ \mathrm{s} \le t < 11\ \mathrm{s}, \\ -0.5\,\mathrm{g}, & t \ge 11\ \mathrm{s}. \end{cases} \tag{70}$$

For $i), ii)$ on the same axes plot the trajectories of the pursuer and evader in blue and red, respectively, and on the same axes plot the pursuer and evader speeds in blue and red, respectively. What is the miss distance in each case?

Problem 4. It is prohibitively slow to run optimal guidance on a missile in real time and thus a computationally cheaper guidance law that uses lessons from optimal guidance is often used in practice instead.

Design a guidance law for the air-to-air missile within the dynamic engagement that does not use real-time optimization. The guidance law can use current and past values of R, $\dot{R}$, $\dot{\beta}$, h_{P}, d_{P}, V_{P}, and γ_{P}. Additionally, the guidance law can use the values of $h_{\mathrm{E}}(0)$ and ~~d~~ $d_{\mathrm{E}}(0)$. Let $n_{z,\mathrm{E}} = -\mathrm{g}$, and simulate the engagement for $0\ \mathrm{s} \leq t \leq 50\ \mathrm{s}$ by using the dynamic differential equations (43) and (46) your guidance law against the 10 scenarios specified by 10 initial conditions in the skeleton code and report the number of detonations (fuzing conditions met). You must 1) clearly explain your guidance law, and 2) plot the pursuer and evader trajectories for each scenario. If your guidance law results in intercepts for more than 3 scenarios, then it performs better than the gravity-corrected proportional guidance law. ~~Your guidance law may not perform better than the gravity-corrected proportional guidance law, and points will be given for clarity of explanation and justifications, and not on the number of successful scenarios.~~

It's okay if your guidance law doesn't perform better than the gravity-corrected proportional guidance law; points will be given for clarity of explanation and justifications, and not on the number of successful scenarios.

Hint: Data from an optimal guidance engagement is provided in `OptimalGuidanceRunData.mat`. *You can hard code maneuvers that the optimal guidance law executed. These hard coded maneuvers can depend on measurements. Do not forget to gravity correct your guidance law.*